Topological Optimization and Methodology for Fabricating Additively Manufactured Lightweight Metallic Mirrors

Michael Stern* and Joseph Bari†

***Massachusetts Institute of Technology, Lincoln Laboratory, MA 02420**
Presently - Massachusetts Institute of Technology, Media Lab, MA 02139
†Massachusetts Institute of Technology, Lincoln Laboratory, MA 02420
Presently – Ball Aerospace, CO 80301

This work is sponsored by the Department of the Air Force under Air Force Contract No. FA8721-05-C-0002. Opinions, interpretations, conclusions and recommendations are those of the author and are not necessarily endorsed by the United States Government.

Abstract

Imaging systems for space and airborne platforms have aggressive Size, Weight and Power (SWaP) requirements. High quality, lightweight optics help enable these types of systems. Today typical light weighting techniques are accomplished through removal of material in the back structure with classical machining and the use of low-density, high-stiffness materials such as beryllium. We present a novel methodology for generating lightweight metallic mirrors that are fabricated by growing an additive manufactured blank, fly cutting the surfaces to be mirrored, and post processing the faces by coating them with electroless nickel and then diamond turning. This process was used in a case study for the development of a topology optimized, low-weight and high-stiffness spinning mirror. The mirror was fabricated with selective laser melting and post processed to deliver optical quality mirror surfaces.

Acknowledgements

We would like to acknowledge MIT Lincoln Laboratory for funding this technology initiative particularly the Engineering Division and the Technology Office Print Lab Initiative. We would also like to thank Maria Yang, Ideation Lab at MIT and the Lincoln Scholars program that provided additional funds to develop design and optimization methods.

Introduction

In engineering system design, there has always been the drive to reduce the SWaP of a system. This is of paramount importance in the development of aircraft and spacecraft, where every additional pound of payload increases the cost of operation over the 30-year life of the aircraft by $40,000, or a spacecraft launch by $10,000 [1,2]. The use of aircraft and spacecraft for surveillance creates a demand for lightweight optics. The benefit of lightweight optics is compounded when the optic is actuated in the system. This is because of a phenomenon called self-weighting where the mass of the optical component drives its own loading through inertia. As a result, lighter mirrors can lead to great reductions of mass in full systems [3,4].

The state of the art in this industry is ULE™, Zerodur™, or beryllium isogrid mirrors. The isogrid design is a standard in which a solid block of material is polished on one side to a mirror surface while the other side is machined with pockets to remove substantial mass yet maintain much of the stiffness [3]. In 2018, when the James Webb Telescope is launched, its main mirror will be comprised of 18 beryllium hexagonal sub components at a target cost of $150M and will have required eight years to complete [5,6].

While the performance of beryllium isogrid mirrors is exceptional, the manufacturing cost and lead times are serious limitations. The cost is very high because of both the rarity of beryllium and the high toxicity of particles produced during fabrication. Many systems instead utilize metal reflective optics made of aluminum due to their ease of processing and low cost as well as system-level design constraints on material ubiquity or mass. There is a great deal of work being done to explore methods to generate lightweight non-beryllium mirrors beyond the typical isogrid design. One of those methods explores the bonding or brazing of aluminum face sheets to aluminum foams to create sandwich panels [7]. This technique creates many challenges of its own due to the bonding, assembly, and risk of delamination. Composite replica molded mirrors are also being investigated, but they require expensive tooling and pose risks from a material longevity standpoint [4].

Additive Manufacturing and Design of End-Use Parts

While additive manufacturing (AM) has existed for 30 years, only in the last decade has Rapid Manufacturing (RM) become widespread. RM is the practice of creating end-use parts by AM, meaning that they will be fully utilized not as prototypes, but as final parts [8]. This transition has been spurred both by the development of better machines and materials and also by more informed designers and more inventive applications.

The increased use of AM for end-use part fabrication has created a need for powerful design tools to effectively deal with increased complexity. As a result, topology optimization has become a popular tool to use when designing for additive manufacturing [9,10]. Topology optimization is a design technique developed in 1988 by Bendsoe and Kikuchi for the generation of optimal material layouts [11,12]. The synergy between topology optimization and additive manufacturing stems from the freeform complex shapes that can be generated and then fabricated respectively by these two processes [13]. One of the most popular industrial software packages used for this purpose is Altair Optistruct. An example of a case study conducted with Altair for metal additive manufacturing was done by Tomlin and Meyer where they worked to reduce the weight of a bracket for the A320 aircraft [14].

The utilization of rapid manufacturing and topology optimization for metallic end-use parts creates the opportunity to fabricate mirrors with far greater geometric complexity than previously possible. The opportunity to fabricate parts with variable density, in which both sparse low-mass regions and solid regions exist, is of high value for optics. Mirrors can be grown with low-mass areas for stiffness and connectivity and solid face sheets for the mirror surfaces, allowing lighter, higher performance mirrors to be created.

Paper Structure

This paper addresses two separate questions. The first, whether additive-manufactured mirror blanks could be post processed to enable high-quality mirror surfaces, comparable to those made conventionally. This question was critical because it would demonstrate the applicability of the proposed finishing method since there were challenges to overcome the non-standard alloys and levels of porosity and bulk metallic properties of the printed material. The second question was how leveraging additive-manufacturing design freedoms could deliver a higher performance mirror. Because the latter question was contingent on the success of the former (creating high-quality mirror surfaces) these two topics will be covered sequentially. We expected that if the viability of the process could be demonstrated, then the design freedom of AM could be applied to the development of novel mirror geometries disrupting typical manufacturing to enable an expansive design space.

Proposed Method

Substrate Fabrication

Given the desire to create highly intricate metallic geometry, Powder Bed Fusion (PBF) was selected for fabrication. PBF is a process where parts are created layer-by-layer by fusing small particles of material together through the selective application of thermal energy. The process metallic powder bed fusion, often creates high residual stresses during part fabrication. Support structures are used anchor the part to the build plate during fabrication and stress relief and then are removed from their build plates. It was decided to test two different technologies within PBF: Electron Beam Melting, where an electron beam is used to create the thermal energy for fusion, and selective laser melting, where a laser beam is used to generate the thermal energy. For Electron Beam Melting an Arcam Q10 machine was used and for Selective Laser Melting an Electro Optical Systems (EOS) M280 machine was used.

Two different materials— titanium and aluminum (specifically Ti6Al4V and AlSi10Mg) — were evaluated for this project. They were selected for their high specific strength, low density, and prevalence in AM. It is important to note that the current generation of commercial Arcam machines are unable to process aluminum; therefore, aluminum was only tested using on the EOS laser based system.

Two artifacts of the PBF process need to be overcome by finishing techniques. First, porosity exists in bulk metallic PBF, where the density is typically 99.5% but not 100.0% [15]. Any voids have the potential to create imperfections in the mirror surfaces. Second, as the surfaces of a PBF part are created, a layer of partially fused powder adheres to the surface, creating a low-density region that must be removed to obtain material of bulk properties [16].

Mirror Finishing Techniques

Metal reflective optical substrates are commonly post-processed to achieve optical characteristics such as flatness, angularity, roughness, and reflectance. The diamond turning process removes small amounts of material to achieve flatness on the order of one micron and surface roughness on the order of one nanometer [17]. Materials with high ferrous content are not readily diamond turned due to extensive tool wear caused by galling and micro-welding. Similarly, materials with a particularly hard or brittle oxide layer lead to tool damage and wear.

The tool dimensional instability and dulling reduce the capabilities of the diamond turning operation. This limits the use of many prevalent metal additive materials, including high silicon content aluminum, titanium alloys, and alloys with high molybdenum content, such as 316 stainless steel.

A thin coating may be applied to a substrate to increase machinability. A coating more tuned to the diamond turning process can be used to preserve tool integrity, reducing dimension instability caused by premature wear and dulling. One such coating is electroless nickel. This coating is readily machined by diamond turning. It also has added optical advantages such as temperature stability, high reflectivity, and resistance to corrosion.

In this project, the substrates produced by AM were post processed to achieve the desired optical characteristics. For this proposed process, initial surface material removal was performed by fly cutting the optical surface with a standard machine tool. The additively manufactured substrate was oversized by up to 0.030 in to compensate for this material removal. This created a more tightly constrained optical geometry, flat to 0.001 in and parallel to 0.002 in, as well as removed the porous surface layer of the part. The optical surface was machined to a surface figure 0.001-0.005 in. smaller than nominal. The part was then heated to 320°F for 18 hours to relieve residual stress from the sintering and machining processes to prevent subsequent material deformation.

After the first machining step, electroless nickel was deposited on to the substrate in a 0.005 in layer to provide a foundation for diamond turning and the application of a subsequent optical coating. This critical step greatly reduced the dependency of the final mirrored surface on the substrate material. Substrate and nickel materials must still be matched to prevent delamination or bimetallic stresses in extreme environments. After the application of electroless nickel the part was then put through a standard diamond turning operation. The diamond-turning tool removed a layer of nickel to create optically suitable surfaces. The final step was the application of an optical coating. Standard optical coating processes were used to tune the desired optical performance. Coatings can include antireflective coatings and diamond-like carbon coatings. For our samples, an AlMgF coating was used to increase reflectance of the mirrors and enhance surface toughness.

Test Samples

To prove the viability of the finishing process, 1 in by 1 in by ¼ in square test samples were fabricated vertically standing on edge, matching the expected orientation of the final mirror faces, and then analyzed. This work was completed by a service bureau with additive manufacturing parameter sets that unfortunately were not made available. Two common AM powder bed metallic processes were used: Electron Beam Melting (EBM) and Selective Laser Melting (SLM) with two common lightweight materials, Ti-64V and AlSi10Mg. Additionally, two separate finishing processes were investigated, shown below in Figure 1.

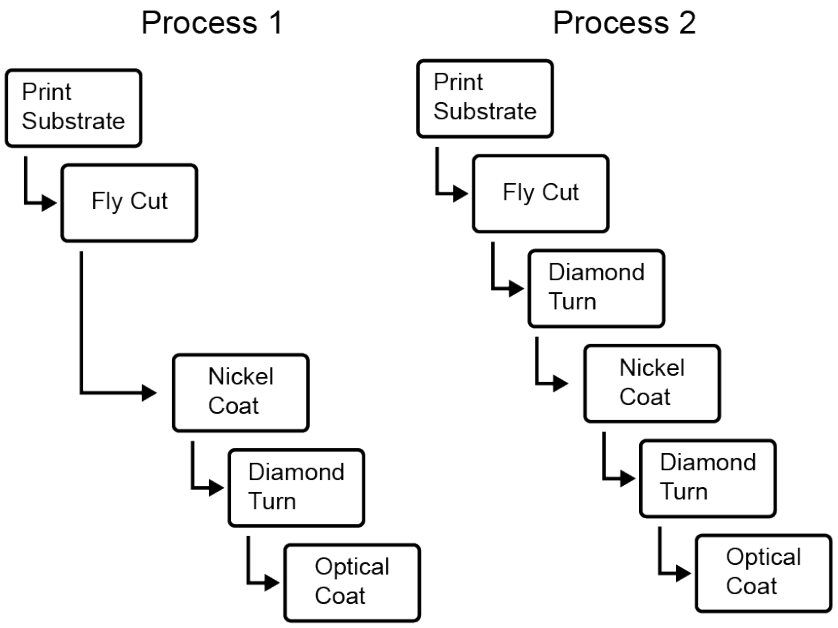

Figure 1: Optical Process Flow Chart, Process 2 shown, process one excludes first diamond turning operation.

For both processes one and two, samples were produced with PBF. They were then machined to mirror surfaces. The differentiating step was included for process two in which the sample was diamond turned prior to coating. For process 2, this additional step was added to aid in the holding the required tolerances of the parts. The samples were next coated with a layer of electroless Nickel. The nickel layer was diamond turned, and the sample was given a final optical coating of AlMgF.

Results

The surface quality of each test sample was inspected using an optical profilometer capable of calculating surface roughness reported through two common metrics (peak-to-valley (PV), the maximum normal distance between a lowest and highest point is measured, and Root Mean Square (RMS), where a weighted average of normal distance between points and the mean surface is measured. These measurements were taken and reported in units of waves at 633 nm. Sample profilometer output is shown in Figure 2. Full results are listed in Table 1.

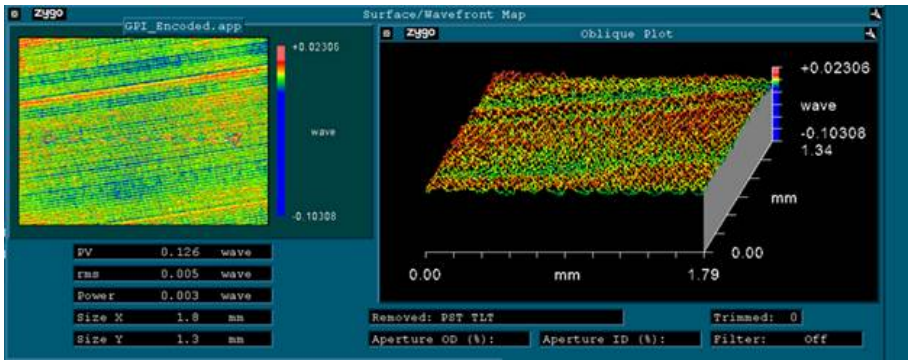

Figure 2: Sample profilometer output of a printed test coupon. A top view (left) and perspective view (right) are shown. The colors represent surface height where peaks are shown in red and valleys in blue.

Peak-to-valley and root mean square measurements were taken to characterize the rugosity of the surface. Optical power was also measured to give an indication of bulk surface figure away from a nominal flat profile. These results are consistent with the surface figures necessary for many optical systems that can currently utilize metal reflective optics. A similar imaging system, for example, would be diffraction limited (ideal image quality) with roughness specifications on the order of 0.2 wave (633nm) PV and 0.013 wave (633nm) RMS, and power specifications on the order of 1 wave (633nm) [18].

Table 1: Optical Properties of Test Samples
Results of finishing process and materials on optical characteristics measured in units of wavelengths at 633 nm. Values that did not meet the optical specifications of the mirror are denoted with *.

Sample Number	**Material**	**AM Process**	**Optical Process**	**PV (wave)** Typ (0.200)	**RMS (wave)** Typ (0.013)	**Power (wave)** Typ (1.000)
1 2 3	AlSi10Mg	DMLS	1	0.126 0.059 0.080	0.005 0.006 0.006	0.003 0.004 0.004
4 5 6	AlSi10Mg	DMLS	2	0.085 0.549* 0.099	0.013 0.015* 0.017*	0.000 0.007 0.011
7 8 9	Ti6Al4V	EBM	1	0.355* 0.103 0.808*	0.005 0.006 0.014*	0.002 0.001 0.007
10 11 12	Ti6Al4V	DMLS	1	0.120 0.180 0.582*	0.011 0.010 0.012	0.014 0.000 0.002

These surface figures would be inadequate for systems with shorter wavelengths or that utilize optical designs dependent on lower surface error for aberration control. Currently, metal optics are not an option for these systems due to limitations of the diamond turning process for both wrought and additively manufactured materials [18].

These results are particularly promising for mid-and long-wave (3000nm-15000nm) infrared imaging applications, in which diffraction limited optical performance is possible with sub-micron surface error. The parallel peaks and valleys evident in Figure 2 are prevalent in all diamond turn test samples and are characteristic of the diamond turning process. This banding is unrelated to the build orientation of the substrate.

Given the small sample size, we did not directly compare the quantitative results here instead we observed that high quality mirror surfaces were generated with both materials and both processes. Both processes, DMLS and EBM, are suitable to create substrates for finishing, as well as both materials tested, AlSi10Mg and Ti6Al4V. Based on these results we affirmatively answer the first question posed "whether additive-manufactured mirror blanks could be post processed to enable high-quality mirror surfaces, comparable to those made conventionally." Additionally, we determined that it seems possible to fabricate mirrors made out of both

AlSi10Mg and Ti6Al4V providing flexibility to design based upon structural constraints of an application.

Spinning Mirror Case Study

The second phase of the project centered on applying the AM mirror surfacing technique to a real-world problem. The problem chosen for this was a high-speed spinning mirror for an imaging application. The system performance drives a requirement for low face deformations under inertial loading from high-speed rotation. This problem was particularly well suited to this methodology because the primary loading of the mirror is self-weighted loading driven by the mass of the mirror itself. Therefore, as mass is cut from the design, the loading is also reduced, providing positive feedback that helps dramatically reduce weight.

Design for AM Mirrors

Driven by the functional requirements for the mirror, topology optimization was selected as the approach to generate the design. Topology optimization is a method for generating optimal material distribution within a given volume subject a certain set of constraints, load conditions and an objective[11]. Often resulting in complex structures, there is a powerful synergy between the shapes generated through this process and the freedom afforded by additive manufacturing [10,19,9]. Traditionally, engineers are taught to carefully consider design for manufacturing, design for assembly, and past designs for inspiration. In order to effectively design for AM, much of this must be put aside given the dramatically different process requirements.

Topology optimization for this project served not only for inspiration as it is often currently used, but also as a way to generate finalized geometry. In order to successfully utilize topology optimization for final geometry generation greater specificity is required both during the formulation of functional requirements and the generation of boundary conditions. A proposed topology optimization workflow is shown in Figure 3.

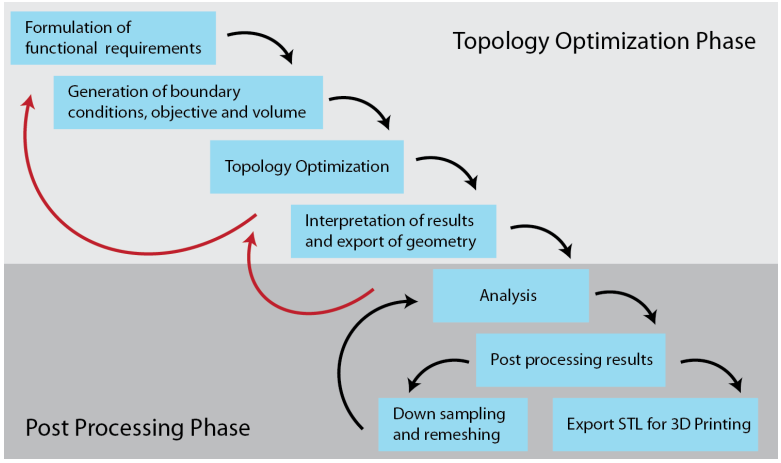

Figure 3: AM Optimization flow chart, with backward red arrows representing the often required reformulation and experimentation.

For this case study Altair's Hyperworks and Optistruct tools were utilized to process the topology optimization. To avoid the reinterpretation of the topology optimized output model from a mesh back into a solid model (an activity that fights complexity), a process was developed instead to edit the mesh directly. This provided two distinct advantages. First, it saved the enormous effort of translating a complex design into a parametric model. Second, it embraced the link between the triangular mesh used in STL description of 3D models with the tetrahedral mesh used for the analysis and optimization. This enabled quicker transition between design and analysis. To further detail the workflow shown in Figure 3 this case study was used to examine each step of the process.

1. Formulation of Functional Requirements
   First, the required characteristics of the part were captured within the specific functional requirements. The mirror was required to spin at a constant rate of 21 Hz about its center axis. The geometry was constrained by the requirement for optical surfaces as well as the mechanical interface with the motor. For system packaging efficiency, the motor that spun the mirror was installed inside of the mirror body connecting with the optic via the hub, as shown in Figure 4. For optical surfaces, deflections of no more than 500 nm across a face under rotational loading were allowable.

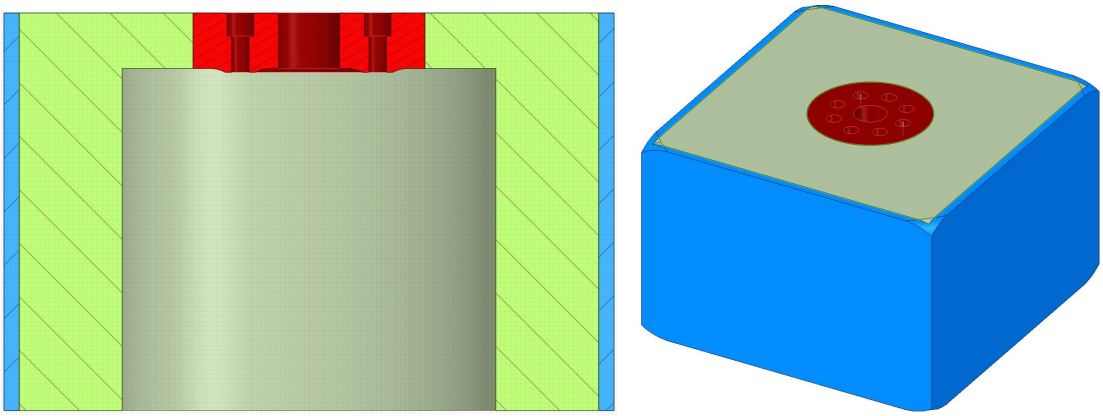

Figure 4: Mirror bounding volume: Red portions defined mechanical interface regions that cannot be modified. Blue portions are mirror faces and cannot be altered. The central void houses the drive motor and is unavailable. Green is the design volume.

2. Generation of Boundary Conditions, Loads, Objective, and Design Volume
   Second, the functional requirements were converted into mathematical representation. The boundary conditions, loads and objective were formulated to be defined in a finite element framework and the design volume to be expressed geometrically and to be split into permanent, non-design, regions and design regions that could be modified by the solver.

Problem Formulation:
Objective:

$$\min(f) = \sum \rho_i$$

Where i is the index of each finite element and ρ is the virtual density

Constraints:

$Displacement\ X_j < 520nm^*$

Where j is the index of each the face elements

*520nm absolute displacement constraint based on 500nm relative (PV) displacement requirement

$Displacement\ Z_k < 90\mu m$

Where k is the index of each the elements on the horizontal surface at the top non-design region

Optimization Input Variables:
Minimum member size constraint: 5.5mm
Discrete (Penalization) Factor: 3.0

Load Cases and Boundary Conditions:
L1, Inertial loading: rotation at 21Hz about the central axis
L2, Z Load: 5MPa pressure applied through to the top face of the non-design region
BC1, Bolted Interface: Elements in bolt hole fixed in all six degrees of freedom
BC2, Symmetry: Elements on symmetry faces fixed in translation normal to symmetry plane

Material Properties:
$E = 70GPa$
$\upsilon = 0.3$
$\rho = 2.67\ {}^{g}/_{cm^3}$

Finite Element Model Details:
Element Type: Second order tetrahedral elements
Element Size: 20,000 approximately 3mm in length
Non-design region: Yellow elements, containing hub elements and mirror faces
Design Region: Green elements, containing interior space between hub and mirror faces
Symmetry: One-eighth model generated through rotation and mirror based translation

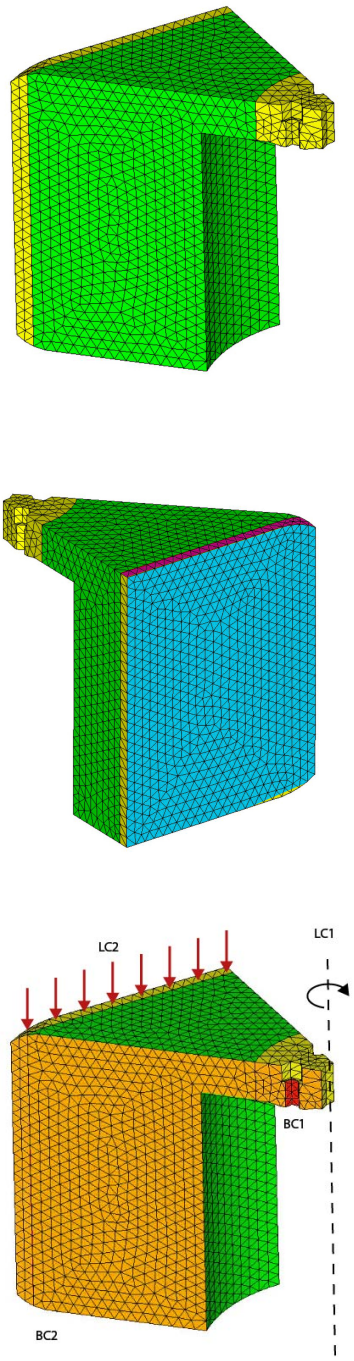

Figure 5: Left mathematical formulation of problem. Right Top: Optistruct finite element model of one-eighth mirror Yellow elements are non-design and cannot be modified while the density of the green elements can be altered by the solver. Right Middle: Blue face highlights nodes included in X displacement constraint. Magenta face highlights nodes included in Z displacement constraint. Right Bottom: Shows model with boundary conditions and loads. Orange faces contain element nodes with symmetry plane boundary condition (note back symmetry plane is not observed) and red faces contain elements nodes with full fixed boundary condition.

3. TO Software Execution

The topology optimization routine was run in Altair Optistruct version 12.0.212 and executed over 80 design iterations until the iteration limit was reached, over approximately 37 minutes.[1] After executing the topology optimization routine, the results were interpreted through additional analysis.

4. Analysis

Additional analysis on the design was run to gain an understanding of how the thresholding and smoothing had affected the design. OSS Smooth within Optistruct was used to threshold and smooth, the design and to reapply the original boundary conditions and load cases. This analysis highlighted deficiencies as well as excess structure in the design. For the mirror the resulting output was then run at various density threshold values. A density threshold of 55% was used supplemented by a feature that allowed lower density connection elements. This connection detection limit was set to 30%. With these settings OSS smooth generated the model corresponding to the left image of Figure 6.

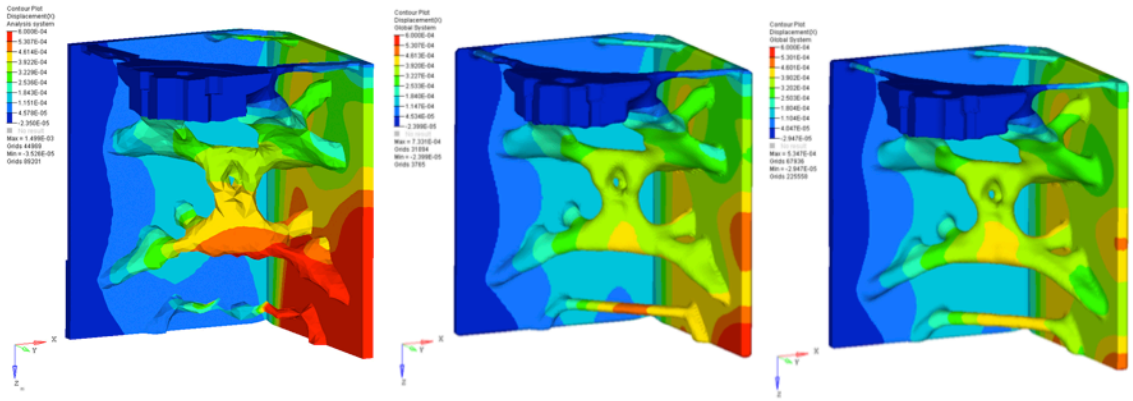

Figure 6: One-quarter mirror model showing displacements normal to the x-face (right); red regions do not meet specifications. Left, initial design directly from OSS Smooth; center generated after single manual design iteration and right, after additional post processing.

While initial performance was out of the required specification, observed as large red displacements in the design, adequate performance in the top half of the design and the kinked beam at the bottom of the design presented an opportunity for direct editing to increase the stiffness of the design rather than increasing the threshold.

5. Post Processing

In order to avoid regeneration of the geometry as a parametric model, the tetrahedral mesh generated during the analysis step was directly used to create an STL file from its surface triangles. This was loaded into a software tool for direct mesh editing and smoothing. The first post processing step was to utilize the symmetries that were taken

[1] Desktop PC with 2.13Ghz Intel Xeon with 12GB RAM.

advantage of in order to simplify the problem to regenerate the full part. A reflection of the one-eighth model in 3-Matic STL generated a one-quarter model that ensured tangency along the reflection plane during the subsequent smoothing. The quarter model was imported into Meshmixer where it was manually modified to straighten the bottom gusset and then locally smoothed.

6. Down Sampling and Remeshing
   The design, in the center of Figure 6, was next exported for reanalysis in Optistruct. During this step, the STL was simplified from approximately 270,000 triangles to 80,000. This expedited the remeshing and analysis. A tetrahedral mesh of approximately 400,000 elements was generated using the surface mesh of the STL to seed it. This increase of model order to transform from 2D mesh to 3D mesh highlights the power of this simplification, which otherwise would have yielded a quarter model with an estimated 1.4 million elements.

   Based on these results the design returned to step 5 and was post processed. The lower of the design was stiffened by adding material to the bottom and middle gussets. After a final reanalysis, the performance in the right image of Figure 6 was achieved and found to be within the specification. The direct modification method used here was highly efficient; both the time required to make these changes and 1.32% increase in mass of the design were minimal. This value can be compared to the alternative, an increase in overall threshold, which resulted in an increase in mass of 7.82%.

7. Export STL for 3D printing
   Finally, after the analysis verified the performance, an STL was exported for 3D printing. The model used for printing was the file generated at the end of step 5, rather than the down sampled design used for the verification. [13]

Results:

Utilizing these methods, we created much lower mass mirrors with functional properties equivalent to that of the traditional ones that had been used. In Figure 7, the two different designs are shown side by side for comparison.

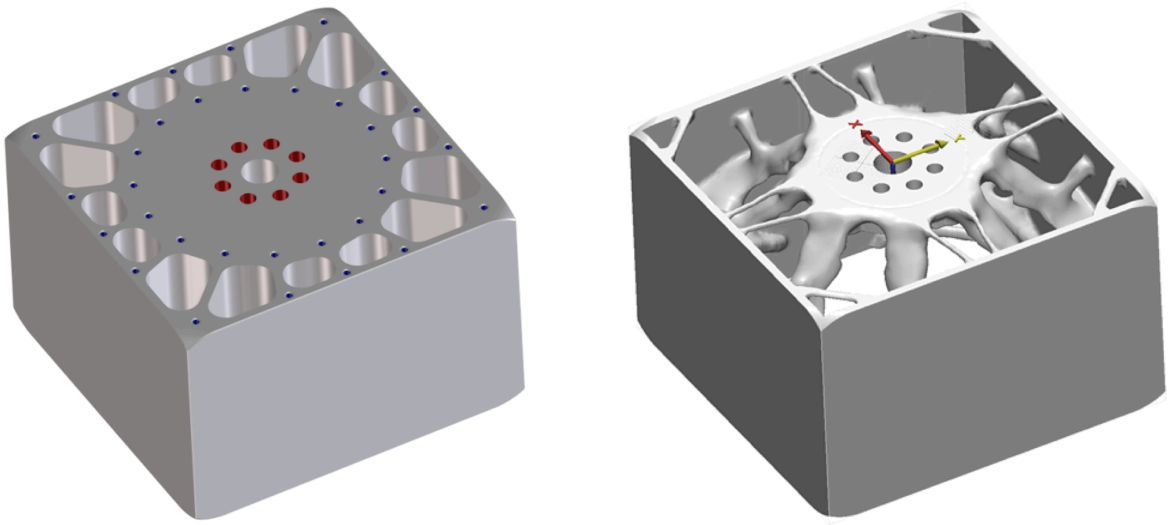

Figure 7: Traditional mirror design on left, the 62% lighter, topology optimized, additive mirror design on right

The AM design for the mirror was 62% lighter than the conventional design with a surface deflection of 420 nm, remaining under the required 500 nm threshold for surface deflection. Both mirrors were manufactured for similar costs and in a similar amount of time. For both mirrors the most resource intensive element was the diamond turning and surface coatings that tend to be the most expense and time consuming part of mirror fabrication.

Conclusion:

Our results indicate that this methodology provides an effective means to fabricate complex, lightweight mirrors. Initial testing showed that a variety of different processes, finishing techniques and materials produced high-quality mirror surfaces on AM substrates. We believe that this is a very promising approach to the fabrication of lightweight mirrors for weight critical applications, particularly for designs in which self-loading is substantial or the mirror must be positioned rapidly. For either of the cases, having a lower weight mirror enables substantial system-level weight reduction. Additionally, in the future, we are interested in the use of this technology to enable cost-effective fabrication and development of free form optics.

In the future, we are interested in conducting further research into this area, exploring larger sample sizes to validate the results from this study, which only examined a small number of artifacts. Finally, we believe it would be valuable to conduct durability testing on these mirrors to ensure that the electroplated coatings remain effective over significant time periods.

Research and development are currently underway to enable printing of Beryllium through the EBM process [20,21]. It is expected that a similar process to the one described in this paper could be applied to a Beryllium mirror using either electroless nickel or gold plating to build up a surface for the mirror finish. While the printing of this toxic material is a challenging task, the use of Beryllium powder to create net shape vacuum pressed blocks is common [22]. This gives some promising indications for AM of Beryllium. Doing so would enable the geometric benefits of AM with the high specific strength of Beryllium to produce very efficient mirrors.

References

[1] 2011, “3D printing - The printed world,” Econ.

[2] NASA, 2015, “Advanced Space Transportation Program: Paving the Highway to Space” [Online]. Available: http://www.nasa.gov/centers/marshall/news/background/facts/astp.html_prt.htm. [Accessed: 15-Apr-2015].

[3] Mayo, J., Dehainauta, L., Be, K., Smithc, S., Kilipatrick, D., Dyer, R., and Rda, L., 2000, “Ultra-Lightweight Optics for Space Applications,” UV, Optical, and IR Space Telescopres and Instruments - SPIE, J. Breckinridge, and P. Jakobsen, eds.

[4] Chen, P. C., Shasha, T. T., Smith, A. M., and Romeo, R., 1998, “Progress in very lightweight optics using graphite fiber composite materials,” Opt. Eng.

[5] Stahl, H. P., 2014, “James Webb Space Telescope (JWST): The First Light Machine” [Online]. Available: http://ntrs.nasa.gov/archive/nasa/casi.ntrs.nasa.gov/20120004008.pdf. [Accessed: 04-Dec-2015].

[6] Leonard, D., 2012, “Mirrors Finished for NASA’s New James Webb Space Telescope.,” Space.com’s Sp. Insid. Columnist. [Online]. Available: http://www.space.com/17202-nasa-james-webb-space-telescope-mirrors.html. [Accessed: 09-Oct-2015].

[7] Conkey, S. B., Lee, C., Chaykovsky, S., Aerospace, S., Rd, P. M., Content, D., Morell, A., Budinoff, J., and Space, G., 2000, “Optimum Design of a Lightweight Mirror Using Aluminum Foam or Honeycomb Sandwich Construction — A Case Study for the GLAS Telescope,” SPIE, pp. 325–332.

[8] Wohlers, T., and Caffrey, T., 2014, Wohlers Report 2014, Wohlers Associates, Fort Collins.

[9] Seepersad, C. C., 2014, “Challenges and Opportunities in Design for Additive Manufacturing,” Mary Ann Liebert, Inc., **1**(1), pp. 10–13.

[10] Brackett, D., Ashcroft, I., and Hague, R., 2011, “Topology optimization for additive manufacturing,” Solid Free. Fabr. Symp., pp. 348–362.

[11] Bendsoe, M. P., and Kikuchi, N., 1988, “Generating optimal topologies in structural design using a homogenization method,” Comput. Methods Appl. Mech. Eng., **71**(2), pp. 197–224.

[12] Bendsoe, M. P., and Sigmund, O., 2003, Topology Optimization: Theory, Methods and Applications, Springer.

[13] Stern, M. L., 2015, “Aligning Design and Development Processes for Additive Manufacturing,” Massachusetts Institute of Technology.

[14] Tomlin, M., and Meyer, J., 2011, “Topology Optimization of an Additive Layer Manufactured (ALM) Aerospace Part,” 7th Altair CAE Technol. Conf. 2011, pp. 1–9.

[15] Buchbinder, D.a*, Schleifenbaum, H.b, Heidrich, S. b, Meiners, W.b, Bültmann, J. ., 2011, “High Power Selective Laser Melting (HP SLM) of Aluminum Parts,” Physics Procedia, pp. 271–278.

[16] Gibson, I., Rosen, D. W., and Stucker, B., 2010, Additive Manufacturing Technologies: 3D Printing, Rapid Prototyping, and Direct Digital Manufacturing, Springer, New York.

[17] Roher, R. L. ., and Evans., C. J., 2009, “Fabrication of Optics by Diamond Turning”. Handbook of Optics. Michael Bass., McGraw Hill Professional, New York.

[18] Kasunic, K., 2011, Optical Systems Engineering, McGraw-Hill Education, New York City.

[19] Campbell, I., Bourell, D., and Gibson, I., 2012, “Additive manufacturing: rapid prototyping comes of age,” Rapid Prototyp. J., **18**(4), pp. 255–258.

[20] Arcam, 2006, “Rapid Manufacturing with Electron Beam Melting (EBM)” [Online]. Available: www.rm-platform.com/index.../313-arcam-presentation-december-2006. [Accessed: 02-Oct-2013].

[21] Horn, T., 2013, “Material Development for Electron Beam Melting” [Online]. Available: http://camal.ncsu.edu/wp-content/uploads/2013/10/Tim-Horn-2013CAMAL.pdf. [Accessed: 15-Feb-2015].

[22] Materion, 2015, “Beryllium Pressing” [Online]. Available: http://materion.com/Technologies/MaterialsProcessing/BerylliumPressing.aspx. [Accessed: 15-Feb-2015].